HHS Public Access

Author manuscript

Gene Ther. Author manuscript; available in PMC 2022 April 20.

Published in final edited form as:

Gene Ther. 2022 April ; 29(3-4): 138–146. doi:10.1038/s41434-021-00255-9.

Membrane-Bound MMP-14 Protease-Activatable Adeno-Associated Viral Vectors for Gene Delivery to Pancreatic Tumors

Susan S Butler[1], **Kenjiro Date**[2], **Takashi Okumura**[2], **Cooper Lueck**[1], **Bidyut Ghosh**[2], **Anirban Maitra**[2], **Junghae Suh**[1,3]

[1)]Department of Bioengineering, Rice University, Houston, TX, USA

[2)]Departments of Translational Molecular Pathology and Pathology, Sheikh Ahmed Center for Pancreatic Cancer Research, The University of Texas MD Anderson Cancer Center, Houston, USA

[3)]Systems, Synthetic, and Physical Biology, Rice University, Houston, TX, USA

Abstract

Adeno-associated virus' (AAV) relatively simple structure makes it accommodating for engineering into controllable delivery platforms. Cancer, such as pancreatic ductal adenocarcinoma (PDAC), are often characterized by upregulation of membrane-bound proteins, such as MMP-14, that propagate survival integrin signaling. In order to target tumors, we have engineered an MMP-14 protease-activatable AAV vector that responds to both membrane-bound and extracellularly active MMPs. This 'provector' was generated by inserting a tetra-aspartic acid inactivating motif flanked by the MMP-14 cleavage sequence IPESLRAG into the capsid subunits. The MMP-14 provector shows lower background transduction than previously developed provectors, leading to a 9.5-fold increase in transduction ability. In a murine model of PDAC, the MMP-14 provector shows increased delivery to an allograft tumor. This proof-of-concept study illustrates the possibilities of membrane-bound protease-activatable gene therapies to target tumors.

Introduction:

One of the most commonly used gene therapy vectors in clinical trials is based on adeno-associated virus (AAV) due to its relative safety and ability to package episomally-expressed single stranded DNA (ssDNA).[1] Two FDA-approved treatments have harnessed AAV's natural tropism to deliver therapeutics: Luxturna transduces the retina using AAV serotype 2 (AAV2) and Zolgensma transduces the central nervous system with AAV serotype 9 (AAV9).[2,3] These therapies rely on the natural infection pathway of the virus for the

Corresponding Author: Junghae Suh (jsuh@rice.edu).

Conflicts of Interest

JS is an employee of Biogen as of August, 2019. AM receives royalties for a pancreatic cancer biomarker test from Cosmos Wisdom Biotechnology, and this financial relationship is managed and monitored by the UTMDACC Conflict of Interest Committee. A.M. is also listed as an inventor on a patent that has been licensed by Johns Hopkins University to ThriveEarlier Detection.

delivery of genetic cargo. Unfortunately, gene therapies have the potential to be cytotoxic to off-target organs.[4] To combat this, controllable and targeted gene therapy vectors are necessary to reduce negative off-target side-effects and limit toxicity. AAV has the capability to be engineered to deliver genetic material only after receiving external inputs.[5] Therefore, AAV is a promising platform for investigating stimulus-responsive gene therapy.

Pancreatic ductal adenocarcinoma (PDAC) continues to have a poor 5-year survival rate (9%).[6] This is attributed to the high amount of extracellular matrix inside of PDAC tumors constricting blood vessels, and thereby promoting chemo- and radiotherapeutic resistance; additionally, the persistence of integrin-signaling cascades in the tumors promote survival.[7,8] Gene therapy may offer a solution for targeting the tumor microenvironment. Yet, as with most tumors, there is not a naturally-occurring virus that will target the PDAC tumor tissue. Therefore, development of viral vectors that target the upregulated signaling cascades present in the tumor could improve outcomes for patients.

Matrix metalloproteinases (MMPs) are normally involved in extracellular matrix remodeling and are an attractive possibility as stimuli for responsive gene therapy systems. This family of enzymes is upregulated in many diseases, including endothelial cancers, such as PDAC.[9,10] Extracellularly-activated MMPs such as MMP-2, −7, and −9 are activated excessively in many diseases, and can leave the disease site. Membrane-bound MMPs that are slower to upregulate, such as MMP-14 (or MT1-MMP), have been known to promote migration and tumorigenesis.[11,12] Therefore, targeting membrane-bound MMPs could be used to target tumors more specifically than harnessing extracellular MMP upregulation alone. To this end, a membrane-bound MMP-activatable AAV vector could be beneficial to target cancers such as PDAC.

Previously, we have developed protease-activatable gene therapy vectors, named provectors, that respond to extracellularly-expressed MMPs .[13-16] Short ‘peptide locks’ were genetically inserted into the AAV9 capsid after residue G453, inhibiting binding of the virus to its primary cell-surface receptor galactose. These peptide locks, consisting of a tetra-aspartic acid inactivating sequence flanked on both sides by MMP-cleavable sequences, have been demonstrated to block receptor binding and prevent transduction until cleaved off the AAV capsid by MMPs.[13] Investigation of the tetra-aspartic acid lock has shown that the four amino acids motif with certain steric and charge based properties is necessary for this inactivation. Increasing the length of the inactivating sequence causes more inactivation prior to receiving the proteolytic input.[14,15] Thus far, only extracellularly released proteases have been investigated as a potential input for the provector technology.

Using rational design, this study investigated targeting of a membrane-bound protease, MMP-14, as the input. The generated provector, called IPES, demonstrates improved switchable transduction *in vitro* compared to the previously developed provectors. We demonstrate that membrane-bound MMP activation is possible, but promiscuity in MMP-14’s cleavage motif results in difficulties developing a provector that is activated solely by MMP-14. In an *in vivo* murine model of PDAC, the IPES provector displays better on-target and lower off-target delivery relative to unengineered capsids.

Materials and Methods

Cloning of IPES Provector and Scrambled Controls

The AAV9 provector mutant was created through T4 Ligase ligation of an annealed DNA insert Integrated DNA Technologies using NgoMIV and KasI restriction cut-sites on A9-453-L001 (VPMS) plasmid developed by Guenther et. al.[13] Plasmid was sequence-validated using an external vendor. Scrambled amino-acid sequences were generated either by randomization of letters using random seed in MATLAB or by reversing the amino-acid sequence (Reverse Scramble). Full scrambled sequences are listed in Figure 3a.

Vector Production and Purification

AAV vectors were produced as previously described.[16] Triple plasmid transfection was performed on HEK293T cells seeded on poly-l-lysine-coated 15 cm plates with (1) a packaging plasmid (pAAV2/9 or provector), (2) a self-complementary GFP (scGFP) or mCherry (pFBAAVmU6mcsCMVmCherrySV40pA, University of Iowa Carver College of Medicine) transgene plasmid, and (3) pXX6-80 helper plasmid using 7.5 μM polyethyleneimine (Polysciences). Virus was separated from the cell lysate using iodixanol gradient purification and concentrated using Amicon 100-kDA molecular weight (MW) cut off filters (Millipore) into GB-PF58 buffer (50mM Tris [pH 7.6], 150mM NaCl, 10mM $MgCl_2$, and 0.001% Pluronic 68).

Vector Titer Determination

Vector titers were determined using quantitative polymerase chain reaction (qPCR) as previously described.[17] A SYBR green master mix (Applied Biosystems) was used with primers against the CMV Promoter (TCACGGGGATTTCCAAGTCTC and AATGGGGCGGAGTTGTTACGA).

Benzonase Protection Assay

Virus was diluted 1:10 in 10x Endo Buffer (15mM $MgCl_2$, 5 mg/ml BSA, and 500 mM Tris [pH8.0]) and DI water. Diluted virus was then incubated with either ≥250 units Benzonase (Millipore) or vehicle buffer (50% Glycerol, 50mM Tris [pH 8.0], 20 mM NaCl and 2 mM $MgCl_2$) for 30 min at 37C and then inactivated with 0.5 μM EDTA for a final EDTA concentration of 12mM. Vector titer of the resulting reaction was determined as described above and normalized to the sham treatment to determine efficacy of genome protection.

Protease Cleavage Assay

MMP-2, MMP-7, MMP-9 and MMP-14 (MT1-MMP) were purchased from Enzo Life Sciences. Concentrated viruses were diluted 1:1 in MMP buffer (50 mM Tris-Cl pH 7.4, 150 mM NaCl, and 5mM $CaCl_2$) and treated with 2.85 μM of enzyme (for a final concentration of 0.31 μM) or sham buffer (50 mM Tris-HCL pH 7.5, 1mM $CaCl_2$, 300 mM NaCl, 5μM $ZnCl_2$, 0.1% Brig-35, and 15% glycerol). After a 21-hour incubation, the reactions were stopped using MMP stop buffer (1xGB with 0.001% Pluronic F-68 and 20mM EDTA).

Silver Stain

VPs were visualized using silver staining. $3.0x10^9$ VG were denatured in NuPAGE LDS Sample Buffer and run on 4%-12% Bis-Tris NuPAGE gel for 2 hours at 110V. Silverquest staining kit (Life Technologies) was used according to manufacturer's instructions and imaged with an Epson scanner.

Western Blotting

To obtain protein extracts, the cell pellets were lysed using M-PER mammalian protein extract reagent (78501, Thermo Fisher Scientific) containing protease (P8340, Sigma) / phosphatase (P5726, Sigma) inhibitor cocktail. Cell lysates were resolved on 4%-12% of Bis-Tris gels and transferred onto nitrocellulose membranes. After incubation with appropriate antibodies (Recombinant Anti-MMP14 antibody [Abcam, ab51074] or Beta-Actin Antibody [Santa Cruz, sc-1616]), blots were developed and visualized with Clarity ECL Western Blotting Substrates (Bio-Rad Laboratories Inc.). The detection of bands was performed using ChemiDoc imaging system (Bio-Rad Laboratories Inc.)

Transduction and Binding Assays

CHO-Lec2 cells were seeded onto poly-L-lysine coated 48 well plates (for transduction) or 24 well plates (for cell binding assays). Once cells were 70% confluent ($2.52x10^5$ cells for transduction and $5.04x10^5$ cells for binding), MOI of 5000 virus per cell was added to serum-free MEMα media (Lonza). For transduction assays, media was replaced with serum containing media after 24 hours. Then 48 hours after virus was added, cells were trypsinized, flow cytometry was performed using Flow FACS Canto II (BD Biosciences), and data was analyzed using FlowJo (BD Biosciences). For binding assays, cells were chilled on ice for 30 minutes prior to adding virus. Once virus was added, cells were incubated on ice for an additional hour to allow for binding. Cells were then carefully washed with cold PBS twice to remove unbound virus and lifted by incubating with Corning CellStripper for 20 minutes at room temperature. DNA was extracted from cells using DNeasy Blood and Tissue Kit (Qiagen) according to manufacturer's instructions for cultured cells. Resultant DNA was diluted 1:10 in salmon sperm, and then qPCR was performed to quantify VGs with the known amount of cellular DNA loaded used as reference between samples.

In Vivo Biodistribution Analysis

AAV vectors packaging pFBAAVmU6mcsCMVmCherrySV40pA (University of Iowa Carver College of Medicine) ($1x10^{11}$ VG) or PBS vector control were injected retro-orbitally, into C57BL/6 female mice, 8 to 12 weeks of age, orthotopically implanted with KPC (LSL-KrasG12D/+) cell line tumors two weeks prior. Mice were maintained and treated in accordance with NIH guidelines. Number of mice injected determined by power analysis and detailed in figure legend. Animals were neither randomized nor blinded. After three weeks, the mice were sacrificed, organs excised and snap frozen. Tissues were homogenized using BEADBUG 3 (Benchmark Scientific). 25 mg of tissue was processed for genomic DNA extraction using DNeasy Blood and Tissue Kit (Qiagen), or for RNA extracting using RNeasy Mini Kit with additional RNase-

Free DNase Set (Qiagen), according to the manufacturer's protocols. RNA was reverse transcribed into cDNA according to the manufacturer's protocol using a 3:1 blend of random hexamers and anchored oligo-dT (Verso cDNA Synthesis Kit; Thermo Fisher Scientific). Resultant cDNA was quantified for mCherry expression via qPCR for mCherry (GAACGGCCACGAGTTCGAGA and CTTGGAGCCGTACATGAACTGAGG) and housekeeping gene 18s (AACCCGTTGAACCCATT and CCATCCAATCGGTAGTAGCG) where the ratio is reported for relative expression. Extracted DNA was analyzed via qPCR for VGs per ng of DNA loaded in 20 μL reaction.

Statistical Analysis

Data analysis was performed in GraphPad Prism 7. As indicated in the figure legends, statistically significant differences of replicates were calculated using either Kruskal-Wallis one-way analysis of variance (ANOVA) or un-paired students t-test with a significance level of 0.05.

Results

Generation of MMP-14-Activatable Variants of AAV9

An MMP-14 targeting mutant virus capsid, herein referred to as IPES for the first four amino acids of its cleavage sequence, was designed by inserting the peptide lock AG-IPESLRAG-G-D4-G-IPESLRAG right after the AAV9 capsid amino acid G453. IPESLRAG is a previously identified consensus sequence for MMP-14.[18] A graphical representation of the AAV subunit proteins with the peptide lock insert is shown in Figure 1a with the insertion after G453 in all three virus proteins (VP): VP1, VP2, and VP3. Approximate molecular weight of each viral protein and their corresponding cleavage fragments are depicted. As with our previous work, four major design criterion were considered for this new provector: (1) the capsid must be able to tolerate the peptide lock insertion and maintain capsid assembly and genome packaging, (2) the peptide lock must be cleaved by MMP-14, (3) the inserted peptide lock must lower transduction in the absence of MMPs (denoted as the "OFF" level of transduction), and (4) the provector must regain its transduction ability after MMP exposure (denoted as "ON" level of transduction).[13]

Provectors form at statistically similar titers (Figure 1b) and are able to protect their genomes similarly to AAV9 (Figure 1c). These results indicate that the peptide lock used to generate the IPES variant is tolerated well by the AAV9 capsid and the new provector is comparable to our previously developed VPMS mutant. Therefore, the first design criterion is satisfied.

AAV9 VPs remains intact after MMP −2, −7, −9, or −14 treatment (Figure 2a). Both IPES and VPMS mutants show VP cleavage in the presence of MMPs, but to different degrees depending on the MMP (Figure 2b). Specifically, VPMS is incompletely cleaved by MMP-2 and IPES is incompletely cleaved by MMP-7 and MMP-9, as faint but visible VP3 bands are observed. However, for both provectors, MMP-14 treatment results in complete disappearance of intact VPs. Therefore, both our new IPES mutant and the previously developed VPMS mutant are reactive to MMP-14, satisfying the second design criterion.

There are two potential explanations for the additional smaller band in MMP-2 lanes. One possibility is that there is more MMP-2 protein in those reactions than other MMP reactions, thereby resulting in an observable band (MMP-2 has expected MW of 40 kDa). This is because we do not add the same MMP protein mass per reaction, but rather we add the required enzymatic activity units to the reactions to obtain an active MMP concentration of 2.85 μM for maximum proteolysis. Prior to each proteolysis experiment, we quantify the activity units in the protease stock via the enzyme activity assay detailed in Judd et. al [16] using a fluorogenic substrate. The mass amount of MMP-2 added to the reactions tended to be higher than for the other MMPs (approximately 5% of total reaction by mass as compared to on average 3% mass amount of other MMPs) due to having lower enzymatic activity values. Therefore, higher MMP-2 mass may be resulting in the observable band on the protein gels. The second possibility is there is an undetermined contaminant in the MMP-2 protease stocks used in our experiments and additional studies, potentially with mass spectrometry, are required to identify the source of the extra band.

In order to test if our provectors have protease-activatable transduction behavior, AAV variants were treated with MMP-9 or MMP-14 and added to CHO-Lec2 cells (Figure 2c). Flow cytometry was used to quantify GFP expression at 48 hours post-transduction (Supplemental Figure S1). Transduction index (TI) is calculated as the percent of GFP-positive cells multiplied by the geometric mean fluorescence intensity of GFP-positive cells (TI = %GFP x gMFI). TI is a linear indicator of virus transduction efficiency and is better than quantifying % GFP positive cells alone which saturates at high MOIs. AAV9 shows a high TI regardless of MMP or sham treatment. VPMS and IPES shows decreased transduction ability (11.6% and 3.1% of AAV9, respectively) until treated with MMPs. Transduction reaches a comparable level between the two provectors after MMP activation regardless of which MMP is used. VPMS displays an average 25.1% and IPES displays an average 29.1% of AAV9 transduction efficiency. The lower background transduction ability of IPES in the sham condition results in it performing with a higher fold activation (9.5-fold) than that of VPMS (2.2-fold). Therefore, both provectors meet the final two design criteria, but IPES shows a better fold-activation compared to VPMS.

We hypothesized the IPES provector binds cells less when in the “OFF” state (*i.e.*, sham treated condition) than the previously developed VPMS provector. To test this hypothesis, we performed a cell binding assay on CHO-Lec2 cells where the provector variants, treated with sham or MMP-14, were incubated with the cells on ice for an hour to allow for virus binding. Cells were washed twice with PBS to remove unbound vector and viral DNA was extracted for qPCR quantification (Figure 2d). Since the numbers of VGs detected in the samples with provector added are significantly above the background level in the PBS vehicle control, the results suggest the provectors bind to cells with or without MMP-14 treatment. After MMP treatment, IPES displays an average 2.4-fold increase in binding and VPMS displays an average 1.7-fold increase in binding, but these differences are not statistically significant. AAV9 demonstrates high cell binding regardless of treatment. Therefore, switchable cell binding ability of the MMP-14 provector appears to play a role in its activatable transduction behavior, but there may be additional factors underlying the difference in IPES “OFF” and “ON” transduction levels *in vitro*.

Generation of Scrambled Sequence Negative Control of Protease-Activatable Variant IPES

Since the IPES provector demonstrates lower “OFF” state background transduction than VPMS, it was carried forward to further experiments. We endeavored to develop a negative control vector for murine studies by inserting different peptide with scrambled sequences (Figure 3a). A relative cleavability score was generated for each of the scrambled sequences by silver stain analysis. If intact VPs were still visible after incubation with MMPs, the sequence was deemed not cleavable by that MMP. Results of this experiment indicate that several scrambled versions of the IPESLRAG cleavage sequence remain susceptible to proteolysis by various MMPs. PEAI, GARL, and IEAP scrambled vectors remain cleavable by MMPs, which make them not ideal negative control vectors (Supplemental Figure S2). The GRPL scrambled vector has the lowest proteolytic susceptibility (Figure 3b), thus we moved forward with this variant as our scrambled control for *in vivo* studies.

Systemic Injection of Provector Leads to Transgene Delivery to KPC PDAC Tumor and Decreased Delivery and Expression in Off-Target Organs

We next investigated the ability of IPES to target sites of cancer in a murine model of PDAC. An orthotopic PDAC model was induced via the surgical injection of KPC cells in the pancreas (Supplemental Figure S3). Compared to subcutaneous tumor models, this orthotopic model offers the advantage of allowing us to test in an immunocompetent mouse that displays histologically similar tumor environment to that of the naturally occurring disease.[19,20] The histological similarity could indicate that the tumor microenvironment is more closely representing the progression of integrin-signaling cascades in tumors that cause MMP upregulation.

Three weeks post virus injection, the IPES-treated group displays significantly higher VG delivery to the tumor and significantly decreased viral delivery to the off-target organs of the liver and heart (Figure 4a). AAV9 displays generally higher VG delivery in all organs but the tumor. The GRPL negative control vector, denoted as scrambled in the figure, shows VG delivery similar to IPES in all organs but the tumor. This result suggests MMP activation is necessary for the provector’s higher VG delivery to the tumor.

Transgene mRNA expression follows the observed decreases in VGs delivered (Figure 4b). AAV9 treatment results in high mCherry mRNA expression in off-target organs. The IPES-injected group displays a 10-fold decrease in mRNA expression in the heart and pancreas compared to that of AAV9, and a 5-fold decrease in expression in the liver compared to that of AAV9 (not statistically significant). IPES displayed a 3-fold increase in mRNA expression in the tumor (statistically significant). The scrambled negative control vector displays low levels of mRNA expression. Non-tumor mice were also injected with AAV9 and IPES vectors (Figure 5). Without tumors, IPES presents lower VG delivery and lower mRNA expression than AAV9 across the organs tested.

Discussion

Effective cancer gene therapy strategies depend on vectors specifically targeting cancer cells while minimizing delivery to off-target organs to limit toxicity. In previous studies, this

has been achieved by using tissue-specific promoters to limit transgene expression to target tissues.[21,22] This approach is not ideal as it leads to much of the injected dose of vector to be sequestered in off-target organs. In this study, we show that a membrane-bound protease stimulus can be used to direct AAV vectors from their normal off-target organs (such as the heart or liver) to a tumor site using a non-specific CMV promoter. In the future, pairing of tissue-specific promotors with tissue-targeting delivery vectors would present an ideal solution for cancer gene therapy.

Membrane-bound proteases, such as MMP-14, have been shown to cooperate with Kras to create the collagen-dense tumor microenvironment in PDAC tumors.[23] In this study, we demonstrated that activation of an AAV9-based provector is achievable by membrane-bound protein MMP-14. When compared to the VPMS provector,[13] the IPES variant displays similar ON transduction but lower OFF transduction. This result suggests that IPES would have lower off-target transduction *in vivo* than VPMS and, thus, it should be the variant of choice when lower levels of off-target delivery is desired for safety reasons.

Interestingly, many randomized versions of the IPES cleavage sequence remain sensitive to proteolysis, suggesting the combination of amino acids in the IPES cleavage substrate is highly MMP reactive. Some sequences do appear resistant to proteolysis by some MMPs (*e.g.*, IEAP in response to MMP-2) even at the supra-physiological concentrations of MMPs used in our proteolysis reactions. MMP-14 has been shown to have lower selectivity and lower reactivity when compared to other MMPs,[18] suggesting it could be difficult to develop a provector that is highly specific to this protease.

In our animal studies, provector IPES shows increased VG delivery to the tumor and decreased delivery to off-target organs. Our scrambled control does not have the same delivery patterns, which suggests susceptibility to MMPs may play a role in vector accumulation in the tumor. Transgene mRNA expression follows similar trends as VG delivery. Interesting, IPES yields 188.5-fold increase in VG delivery but only 2.5-fold increase in mCherry transgene expression in the tumor. One would expect that higher VG delivery would lead to a similar-fold increase in transgene expression. We previously observed similar findings where the correlation is weaker than expected between VG delivery and transgene expression.[13, 25] One potential explanation is provectors may be sufficiently activated to bind to factors in the tumor microenvironment but not enough to successfully internalize into and transduce cells. Another explanation is the provectors may be sequestered by phagocytic cells in the tumor microenvironment, preventing transgene expression. Additional future studies are required to fully understand the mechanism behind these results. Overall, both mCherry mRNA expression and VG delivery results suggest on-target tumor gene delivery and decreased off-target gene delivery by the IPES provector.

As a delivery platform this provector could be used to deliver suicide genes or immunotherapies. In terms of suicide genes, AAV-mediated delivery of herpes simplex virus type-1 thymidine kinase (HSVtk) and ganciclovir (GCV) has shown promise when combined with radiation therapy.[26] Immune checkpoint inhibitors, such as Nivolumab [27], and tumor necrosis factor (TNF)-related apoptosis-inducing ligand (TRAIL/Apo2L)[28] have been used previously with AAV systems to target tumors. In combination with a tumor

targeting capsid, these cancer therapy transgenes offer the possibility of being enhanced treatments for PDAC.

Conclusion

We present an AAV-based provector that is activatable by membrane-bound protease MMP-14. We demonstrate the provector has increased delivery to PDAC tumors in an immunocompetent murine model, which opens the door to future work using the provector to deliver therapeutic transgenes. Engineering of AAV capsids is a promising avenue to lower toxicity due to off-target delivery. Furthermore, this technology could serve as a template to target other membrane-bound proteases, creating potential for use in other therapeutic applications. Activatable vectors can allow for more controlled therapies as we continue to explore the application of viral gene therapy.

Supplementary Material

Refer to Web version on PubMed Central for supplementary material.

Acknowledgements

We acknowledge University of North Carolina at Chapel Hill Gene Therapy Center Core for providing us with pXX6-80 and scAAV2-CMV-GFP, the University of Pennsylvania Vector Core for providing us with pAAV2/9, and the University of Iowa Vector Core for providing us with ITR-CMV-mCherry.

Funding Information

NIH (R01CA207497) to JS, NCI MD Anderson/Rice Cancer T32 Fellowship 5T32CA196561-05 to SB, and NIH (R01CA220236 and R01CA218403) to A.M.

REFERENCES

(1). Samulski R, Muzyczka N AAV-Mediated Gene Therapy for Research and Therapeutic Purposes. Annu. Rev. Virol 2014; 1 (1), 427–451. [PubMed: 26958729]

(2). Bi L Summary Basis for Regulatory Action -Luxturna. Food and Drug Administration (FDA), May 24, 2019.

(3). Byrnes A Summary Basis for Regulatory Action - Zolgensma. Food and Drug Administration (FDA), May 24, 2019.

(4). Xiong W, Wu D, Xue Y, Wang S, Chung M, Ji X et al. AAV Cis-Regulatory Sequences Are Correlated with Ocular Toxicity. Proc. Natl. Acad. Sci. U.S.A 2019, 116 (12), 5785–5794. [PubMed: 30833387]

(5). Evans A, Thadani N, Suh J. Biocomputing Nanoplatforms as Therapeutics and Diagnostics. J. Control. Release Off. J. Control. Release Soc 2016, 240, 387–393.

(6). Siegel R, Miller K, Jemal A. Cancer Statistics, 2020. CA. Cancer J. Clin 2020, 70 (1), 7–30. [PubMed: 31912902]

(7). Tian C, Öhlund D, Rickelt S, Lidström T, Huang Y, Hao L et al. Cancer-Cell-Derived Matrisome Proteins Promote Metastasis in Pancreatic Ductal Adenocarcinoma. Cancer Res. 2020.

(8). Cid-Arregui A, Juarez V. Perspectives in the Treatment of Pancreatic Adenocarcinoma. World J. Gastroenterol. WJG 2015, 21 (31), 9297–9316. [PubMed: 26309356]

(9). Ellenrieder V, Alber B, Lacher U, Hendler S, Menke A, Boeck W et al. Role of MT-MMPs and MMP-2 in Pancreatic Cancer Progression. Int. J. Cancer 85 (1), 14–20. [PubMed: 10585576]

(10). Jiang W, Zhang Y, Kane K, Collins M, Simeone D, Di Magliano M et al. CD44 Regulates Pancreatic Cancer Invasion through MT1-MMP. Mol. Cancer Res. MCR 2015, 13 (1), 9–15. [PubMed: 25566991]

(11). Cepeda M, Pelling J, Evered C, Williams K, Freedman Z, Stan I et al. Less Is More: Low Expression of MT1-MMP Is Optimal to Promote Migration and Tumourigenesis of Breast Cancer Cells. Mol. Cancer 2016, 15.

(12). Vihinen P, Kähäri V. Matrix Metalloproteinases in Cancer: Prognostic Markers and Therapeutic Targets. Int. J. Cancer 99 (2), 157–166. [PubMed: 11979428]

(13). Guenther C, Brun M, Bennett A, Ho M, Chen W, Zhu B et al. Protease-Activatable Adeno-Associated Virus Vector for Gene Delivery to Damaged Heart Tissue. Mol. Ther 2019 27(3) 611–622. [PubMed: 30772143]

(14). Chen M, Robinson T, Suh J. Longer Inactivating Sequence in Peptide Lock Improves Performance of Synthetic Protease-Activatable Adeno-Associated Virus. ACS Synth. Biol 2019, 8 (1), 91–98. [PubMed: 30614703]

(15). Robinson T, Judd J, Ho M, Suh J. Role of Tetra Amino Acid Motif Properties on the Function of Protease-Activatable Viral Vectors. ACS Biomater. Sci. Eng 2016, 2 (11), 2026–2033. [PubMed: 29721519]

(16). Judd J, Ho M, Tiwari A, Gomez E, Dempsey C, Van Vliet K et al. Tunable Protease-Activatable Virus Nanonodes. ACS Nano 2014, 8 (5), 4740–4746. [PubMed: 24796495]

(17). Ho M, Adler B, Torre M, Silberg J, Suh J. SCHEMA Computational Design of Virus Capsid Chimeras: Calibrating How Genome Packaging, Protection, and Transduction Correlate with Calculated Structural Disruption. ACS Synth. Biol 2013, 2 (12), 724–733. [PubMed: 23899192]

(18). Turk B, Huang L, Piro E, Cantley L. Determination of Protease Cleavage Site Motifs Using Mixture-Based Oriented Peptide Libraries. Nat. Biotechnol 2001, 19 (7), 661. [PubMed: 11433279]

(19). Li J, Qian W, Qin T, Xiao Y, Cheng L, Cao J et al. Mouse-Derived Allografts: A Complementary Model to the KPC Mice on Researching Pancreatic Cancer In Vivo. Comput. Struct. Biotechnol. J 2019, 17, 498–506. [PubMed: 31011408]

(20). Erstad D, Sojoodi M, Taylor M, Ghoshal S, Razavi A, Graham-O'Regan K et al. Orthotopic and Heterotopic Murine Models of Pancreatic Cancer and Their Different Responses to FOLFIRINOX Chemotherapy. Dis. Model. Mech 2018, 11 (7).

(21). Chen S, Johnston J, Sandhu A, Bish L, HovHannisyan R, Jno-Charles O et al. Enhancing the Utility of Adeno-Associated Virus Gene Transfer through Inducible Tissue-Specific Expression. Hum. Gene Ther. Methods 2013 24(4), 270–278. [PubMed: 23895325]

(22). Pacak C, Sakai Y, Thattaliyath B, Mah C, Byrne B. Tissue Specific Promoters Improve Specificity of AAV9 Mediated Transgene Expression Following Intra-Vascular Gene Delivery in Neonatal Mice. Genetic Vaccines and Therapy 2008. 6(13).

(23). Krantz S, Shields M, Dangi-Garimella S, Cheon E, Barron M, Hwang R et al. MT1-MMP Cooperates with KrasG12D to Promote Pancreatic Fibrosis through Increased TGF-β Signaling. Mol. Cancer Res. MCR 2011, 9 (10), 1294–1304. [PubMed: 21856775]

(24). Kozera B, Rapacz M. Reference Genes in Real-Time PCR. J. Appl. Genet 2013, 54 (4), 391–406. [PubMed: 24078518]

(25). Tong J, Evans A, Ho M, Guenther C, Brun M, Judd J et al. Reducing off target viral delivery in ovarian cancer gene therapy using a protease-activated AAV2 vector platform. J Control Release. 2019, 307:292–301 [PubMed: 31252037]

(26). Kanazawa T, Mizukami H, Okada T, Hanazono Y, Kume A, Nishino H et al. Suicide Gene Therapy Using AAV-HSVtk/Ganciclovir in Combination with Irradiation Results in Regression of Human Head and Neck Cancer Xenografts in Nude Mice. Gene Ther. 2003, 10 (1), 51–58. [PubMed: 12525837]

(27). Reul J, Frisch J, Engeland C, Thalheimer F, Hartmann J, Ungerechts G et al. Tumor-Specific Delivery of Immune Checkpoint Inhibitors by Engineered AAV Vectors. Front. Oncol 2019. 9(52).

(28). Jiang M, Liu Z, Xiang Y, Ma H, Liu S, Liu Y et al. Synergistic Antitumor Effect of AAV-Mediated TRAIL Expression Combined with Cisplatin on Head and Neck Squamous Cell Carcinoma. BMC Cancer 2011, 11 (54).

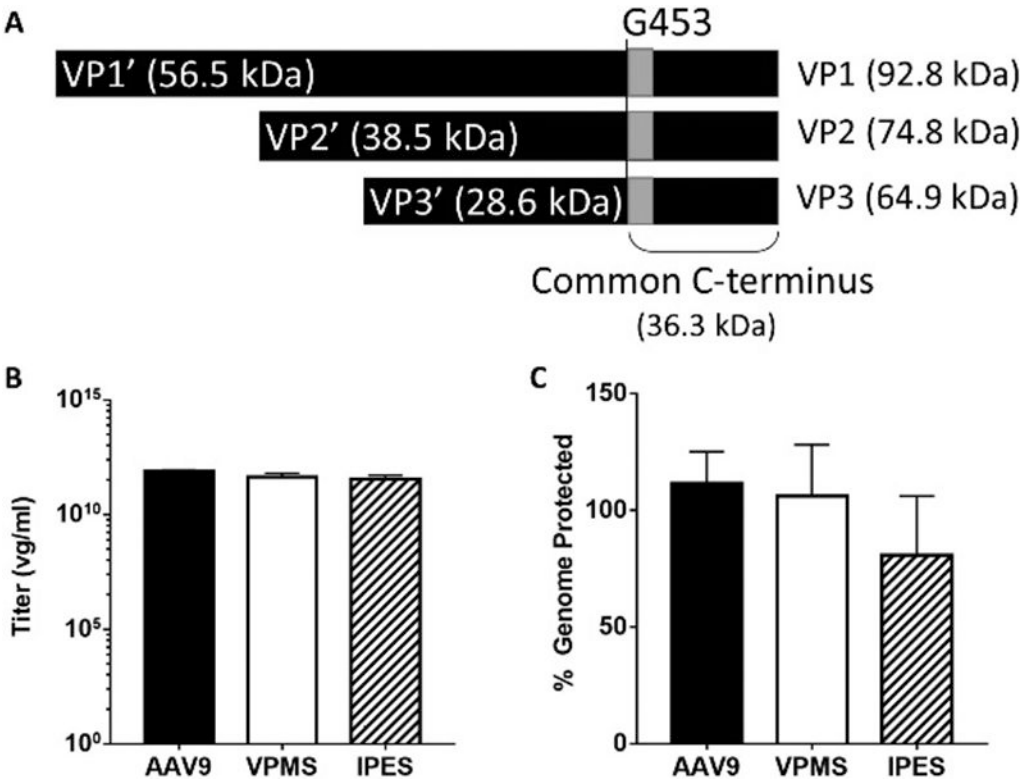

Figure 1.

Provector design and production characterization. A) Peptide lock is inserted after G453 in AAV9 capsid proteins. When exposed to MMPs, VPs are cleaved resulting in protein fragments of four different MWs - VP1', VP2', VP3' and a common C-terminal region. Approximate sizes of each of these protein fragments are shown with the total size of each VP listed on the right. B) Vector production titer of different virus capsids with the same virus genome quantified via qPCR. N=3 independent virus batches, and n=3 technical replicates for qPCR. One-way ANOVA was performed and no statistical difference was determined. Error bars are SEM. C) Benzonase genomic protection assay. Vector samples were treated with benzonase to degrade unprotected viral genomes. After neutralization of the nuclease, virus capsids were denatured and remaining genomes were quantified via qPCR. Percent genome protected is a fraction of genomes in the benzonase-treated sample as compared to number of genomes in the sham sample. N=2 independent experiments and n=3 technical replicates for qPCR. One-way ANOVA was performed and no statistical difference was determined. Error bars are SEM.

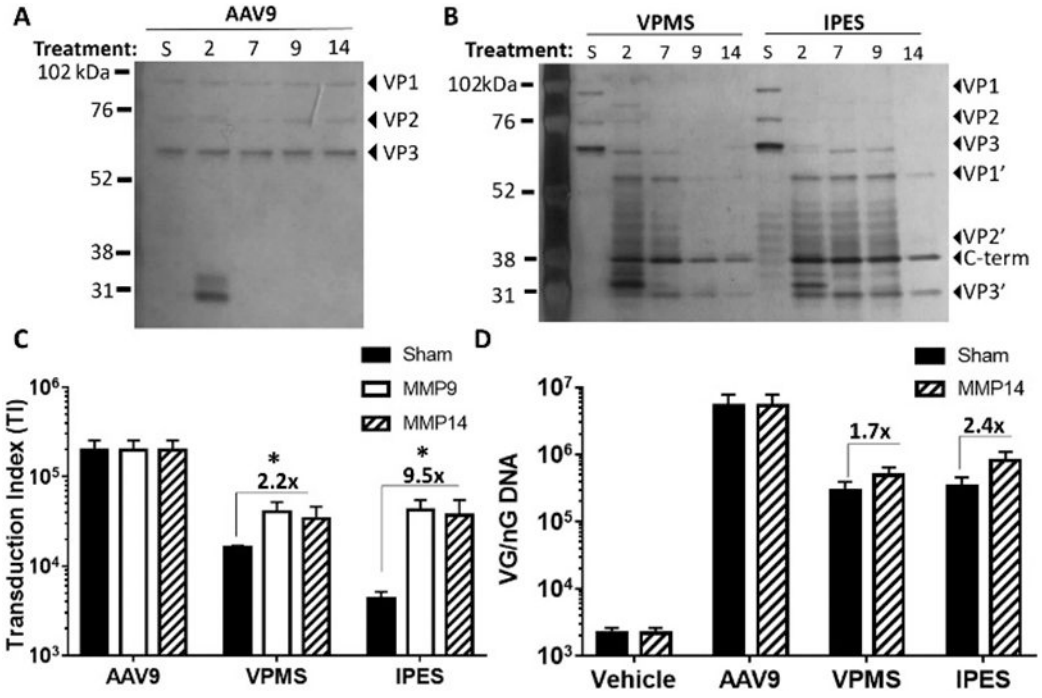

Figure 2.

In vitro performance of IPES provector. A) Silver stain of denatured AAV9 capsid does not display proteolytic fragments when treated with MMP −2, −7, −9, −14, or sham buffer. Intact VPs are visible at their proper sizes indicating the native capsid does not respond to the proteases. B) Silver stain of provectors VPMS and IPES treated with MMP −2, −7, −9, −14, or sham buffer. Disappearance of VP1, VP2, and VP3 bands and appearance of cleavage fragments (VP1', VP2', VP3', and C-term) indicate both provectors are capable of being activated by the MMPs tested. C) Provector transduction behavior in vitro. Vectors were treated with MMPs or sham buffer and added to CHO-Lec2 cells at an MOI of 5000 Viral Genomes (VG) per cell. N=3 independent experiments in n=2 technical replicates. Error bars SEM. One-way ANOVA was performed. * $p<0.05$. D) Cell binding assay. Vectors were treated with sham buffer or MMP-14, added to CHO-Lec2 cells at an MOI of 5000, and incubated for 30 min on ice. Cells were harvested and number of VGs were quantified via qPCR and normalized to total DNA. Provectors have modestly higher binding when MMP treated, with IPES having slightly higher binding than VPMS. N=2 independent experiments in n=3 technical replicates. One-way ANOVA was performed.

A

Scrambled Sequence	Scramble Method	Relative Cleavability
PEAIRLGS	Randomized	+++
GARLSEPI	Reverse Scramble	++
IEAPGRSL	Randomized	+
GRPLIEAS	Randomized	-

Each + indicates cleaved readily by a protease. (Max = 4)

B

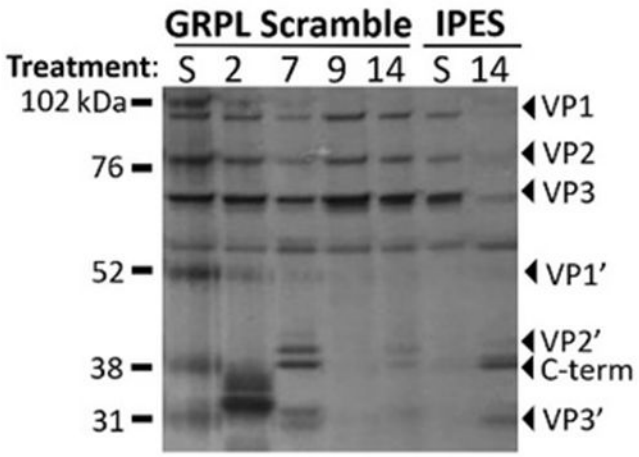

Figure 3.

Development of negative control vector with scrambled protease cleavage sequence. A) Amino acid sequences tested to develop a scrambled negative control vector. Relative cleavage determined by silver stain after 21-hour incubation with MMPs −2, −7, −9, or −14 with each '+' indicating degree of activation by MMPs (+++ cleaved by 3 of 4 MMPs tested, ++ cleaved by 2 of 4 MMPs, + cleaved by 1 of 4 MMPs, - not cleaved by MMPs tested). GRPL variant was selected for animal studies. B) Representative silver stain of scrambled design provector GRPL treated with MMP −2, −7, −9, −14, or sham buffer (S). GRPL variant shows intact viral proteins after MMP treatment.

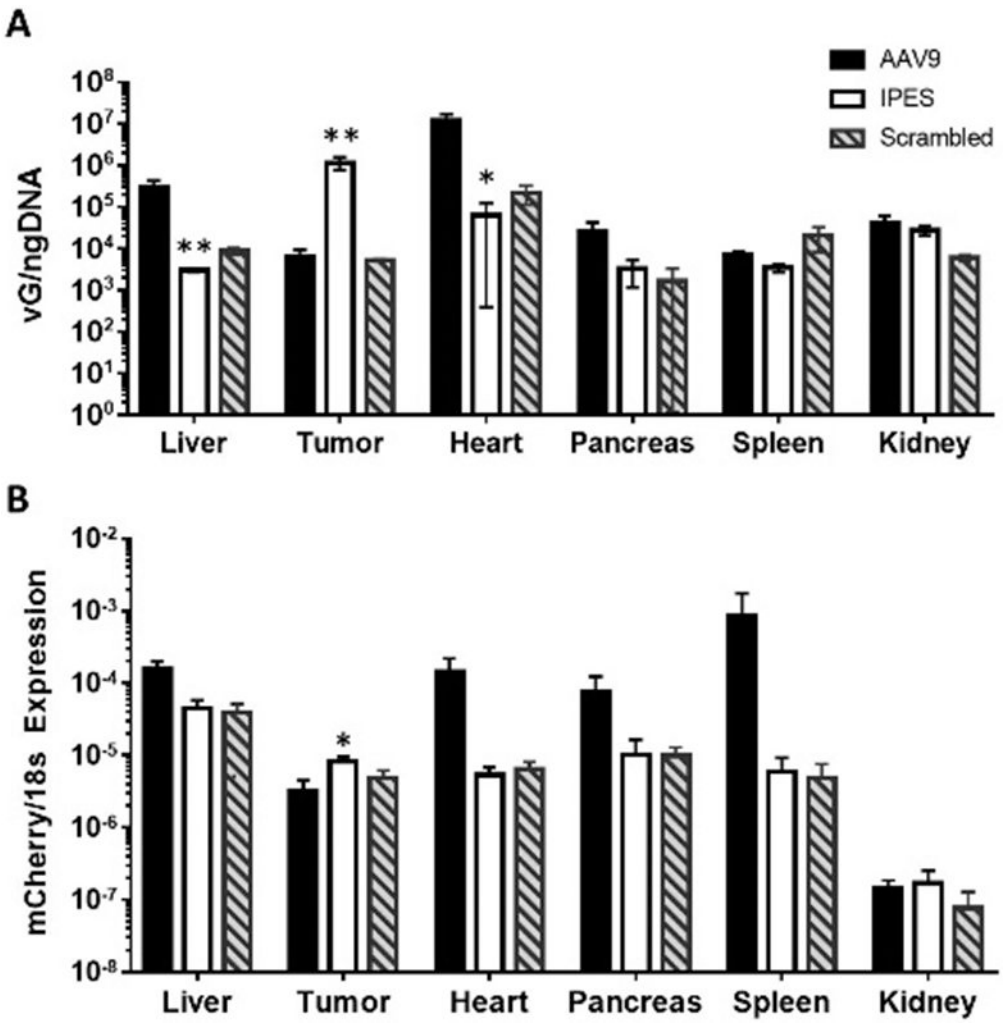

Figure 4.

In vivo performance of provectors in murine model of PDAC. A) IPES provector has increased VG delivery to tumor with decreased delivery to liver and heart. Organs were harvested 21 days following virus injection and genomic DNA was extracted. VG were quantified via qPCR in triplicate and normalized to total DNA. Error bars are SEM. AAV9 and IPES N=6 animals, GRPL Scramble N=3 animals. One-way ANOVA was performed. * $p<0.05$, ** $P<0.005$. B) IPES provector shows increased expression of CMV-mCherry reporter transgene in the tumor. 21 days following virus injection, organs were harvested and RNA was extracted. mCherry mRNA was quantified via qPCR and normalized to 18s mRNA in triplicate. Error Bars are SEM. AAV9/IPES N=6 independent mouse samples, GRPL Scramble N=3 independent mouse samples, n=3 technical replicates per sample. One-way ANOVA was performed. * $p<0.05$.

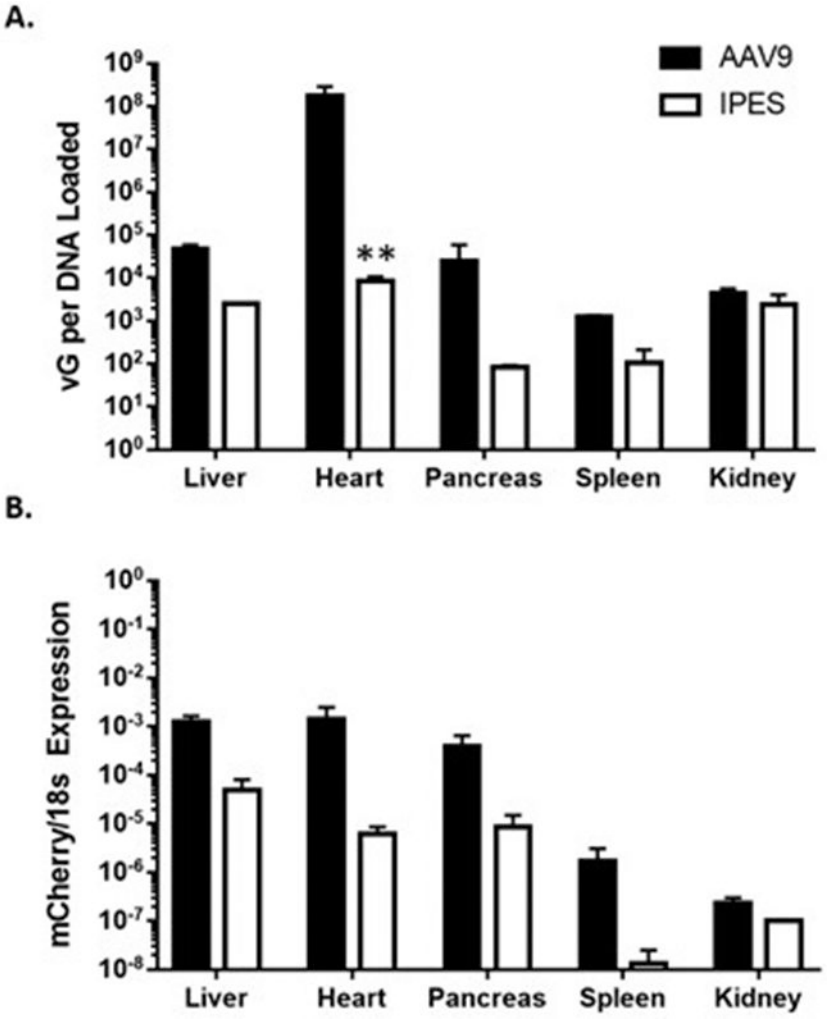

Figure 5:

Non-Tumor Mouse *In Vivo* Performance of Provector. **A)** IPES vector shows decreased VG delivery in heart and several other off-target organs. 21 days following virus injection, organs were harvested and DNA was extracted. VGs were quantified via qPCR in triplicate and normalized to total DNA. Error bars are SEM. **B)** IPES vector shows decreased transgene mRNA expression compared to AAV9 in sampled organs. 21 days following virus injection, organs were harvested and RNA was extracted. mCherry mRNA was quantified via qPCR and normalized to 18s mRNA in triplicate. Error Bars are SEM. N=2 animals, n=3 technical replicates per sample. Students t-test was performed. ** $p<0.05$.